Journal of Molecular Structure 1123 (2016) 162–170

Contents lists available at ScienceDirect

Journal of Molecular Structure

journal homepage: http://www.elsevier.com/locate/molstruc

Effective DNA binding and cleaving tendencies of malonic acid coupled transition metal complexes

Narayanaperumal Pravin, Ponnukalai Ponya Utthra, Ganesan Kumaravel, Natarajan Raman*

Research Department of Chemistry, VHNSN College, Virudhunagar 626 001, India

ARTICLE INFO

Article history:
Received 6 May 2016
Received in revised form
9 June 2016
Accepted 9 June 2016
Available online 13 June 2016

Keywords:
Intercalation
DNA binding
Fluorescence
Antimicrobial activity
DNA cleavage
1,10-Phenanthroline

ABSTRACT

Eight transition metal complexes were designed to achieve maximum biological efficacy. They were characterized by elemental analysis and various other spectroscopic techniques. The monomeric complexes were found to espouse octahedral geometry and non-electrolytic nature. The DNA interaction propensity of the complexes with calf thymus DNA (CT-DNA), studied at physiological pH by spectrophotometric, spectrofluorometric, cyclic voltammetry, and viscometric techniques revealed intercalation as the possible binding mode. Fascinatingly, the complexes were found to exhibit greater binding strength than that of the free ligands. A strong hypochromism and a slight red shift were exhibited by complex **5** among the other complexes. The intrinsic binding constant values of all the complexes compared to cisplatin reveal that they are excellent metallonucleases than that of cisplatin. The complexes were also shown to reveal displacement of the ethidium bromide, a strong intercalator using fluorescence titrations. Gel electrophoresis was used to divulge the competence of the complexes in cleaving the supercoiled pBR322 plasmid DNA. From the results, it is concluded that the complexes, especially **5**, are excellent chemical nucleases in the presence of H_2O_2. Furthermore, the *in vitro* antimicrobial screening of the complexes exposes that these complexes are excellent antimicrobial agents. Overall the effect of coligands is evident from the results of all the investigations.

1. Introduction

DNA is generally the primary intracellular target of anticancer drugs, and their efficiency is exerted through the binding ability of these compounds to DNA. This is the core behind the design and discovery of new and more efficient drugs [1]. Presently, the scientists are focusing on the syntheses and interactions of metal complexes with DNA along with studying their biological applications. This has been an active field of research since the serendipitous discovery of cisplatin and its success despite the side effects. Cisplatin is one of the leading metal-based drugs targeting DNA, widely used in the treatment of cancers especially testicular and ovarian cancers. Nevertheless, the limitations of its usage despite its clinical success are known to originate from its binding mode with DNA and the formation of covalent cross-links [2]. Therefore, the attention of the researchers has been diverted on designing a new design strategy that focuses mainly on synthesis of new metal-based drugs with more-efficacious, target-specific, less-toxic and non-covalent DNA binding [3]. The tendency of metal complexes to interact and bind with DNA (non-covalently) through electrostatic interactions, groove binding and intercalation is a familiar concept [4]. On the basis of these DNA interactions, particularly intercalation draws considerable interest due to its strong binding ability which helped in the development of various applications in cancer therapy and molecular biology [5]. The intercalating ability of the metal complex depends on the type of metal and the structure of the ligand designed [6]. Hence, in the context of design and synthesis of metal complexes that can bind to DNA in the mode of intercalation much attention has been focused on the selection of metal ions and the design of ligands.

In this regard, transition metal ions play a pivotal role in a vast number of diverse biological processes, and their metal complexes have been widely exploited, since their spectral, electrochemical, magnetic and catalytic signatures are unique along with the fact that one can tune the DNA interaction of a metal complex by changing the ligand environment [7]. In the past decades, several

* Corresponding author.
E-mail addresses: pravinknp2012@gmail.com (N. Pravin), ramchem1964@gmail.com (N. Raman).

http://dx.doi.org/10.1016/j.molstruc.2016.06.034
0022-2860/

transition metal complexes were reported owing to their fascinating ability to interact with nucleic acids fabricating them to be DNA intercalative binders as well as DNA cleavers [8]. These effective abilities of the metal complexes enthralled the researchers and fuelled them to research upon such binding interactions with DNA [9] and proteins [10–12] with the promise of varied applications that might be helpful in developing a successful probe or anticancer drug. Moreover, the interaction of complex with DNA causes an agitation due to the localized MLCT (metal to ligand charge transfer transition) which makes the complexes colored. This particular alteration is important which is ideal in providing a spectroscopic probe.

Throughout the literature, among the reported metal complexes, Schiff base transition metal complexes and their design and characterization of biological activity are prominent. Many Schiff base metal complexes having interesting traits in the medicinal and biological activity were previously reported [13–15]. The present work is designed based on the nature of co-ligands used and the geometrical orientation of the complex formed, as they play a vital role in enhancing the DNA-metal complex interactions [16] as an improvement from our previously reported works [17]. Thus, conveying the importance of the ligands in a metal complex, the same has been proved by experimental data reported in this work.

Throwing light on the above facts, we herein report the synthesis, characterization, DNA binding, DNA cleavage (in the presence of H_2O_2) and antimicrobial studies of a series of novel octahedral complexes containing 1,10-phenanthroline and 2,2′-bipyridyine as ancillary ligands. The compounds are Knoevenagel condensate Schiff base complexes with Cu(II), Co(II), Ni(II) and Zn(II) as central metal ions. The obtained results are valuable for further research in crafting and developing effective antimicrobial agents and novel DNA probes so as to meet the demands of the researchers in search of an effective drug.

2. Experimental protocols

The materials and methods, DNA binding, cleavage and antimicrobial procedures are included in the Supplementary file (S1).

2.1. Synthesis of metal complexes

The Schiff base ligand **L** was synthesized using a method previously reported by us [18]. The Schiff base L (5 mmol) was dissolved in ethanol and to this solution, a solution of M(II) chloride (5 mmol) (M = Cu, Co, Ni, Zn) in ethanol was added dropwise while stirring continuously. After the reaction for 1 h at 60 °C, a solution of malonic acid (5 mmol) in ethanol was added. The reaction solution was then refluxed for 2 h. To the resultant mixture, 1,10-phenanthroline/2,2′-bipyridine (5 mmol) was added slowly and the reaction solution was magnetically stirred and refluxed in a rotamantle for 3 h. The reaction mixture was then cooled to an ambient temperature and the obtained solid was filtered, washed with diethyl ether and finally dried in *vacuum*. The outline of the synthesis of the metal complexes is given in Scheme 1.

[CuL(MA)(bpy)] (**1**) Yield: 77%, Anal. Calc. for $C_{37}H_{32}CuN_4O_4$: C, 67.3; H, 4.8; Cu, 9.6; N, 8.4%; Found C, 67.1; H, 4.6; Cu, 9.4; N, 8.2%. IR data (KBr, cm^{-1}); 1602 ν(C=N); 1521 ν(−HC=C); 443 (M−N), 528 ν(M−O). MS *m/z* (%): 659 [M^+]. Λ_M 10^{-3} (ohm^{-1} cm^2 mol^{-1}) = 19.1. λ_{max} (nm) in DMF, 720, 380, 316. μ_{eff} (BM): 1.83.

[CoL(MA)(bpy)] (**2**) Yield: 72%, Anal. Calc. for $C_{37}H_{32}CoN_4O_4$: C, 67.7; H, 4.9; Co, 8.9; N, 8.5%; Found C, 67.4; H, 4.5; Co, 8.7; N, 8.2%. IR data (KBr, cm^{-1}); 1597 ν(C=N); 1515 ν(−HC=C); 437 (M−N), 518 ν(M−O). MS *m/z* (%): 655 [M^+]. Λ_M 10^{-3} (ohm^{-1} cm^2 mol^{-1}) = 14.2. λ_{max} (nm) in DMF, 667, 578, 441. μ_{eff} (BM): 4.85.

[NiL(MA)(bpy)] (**3**) Yield: 79%, Anal. Calc. for $C_{37}H_{32}N_4NiO_4$: C, 67.8; H, 4.9; N, 8.5; Ni, 8.9%; Found C, 67.5; H, 4.7; N, 8.2; Ni, 8.8%. IR data (KBr, cm^{-1}); 1584 ν(C=N); 1527 ν(−HC=C); 440 (M−N), 524 ν(M−O). MS *m/z* (%): 654 [M^+]. Λ_M 10^{-3} (ohm^{-1} cm^2 mol^{-1}) = 20.4. λ_{max} (nm) in DMF, 683, 582, 427. μ_{eff} (BM):3.15.

[ZnL(MA)(bpy)] (**4**) Yield: 75%, Anal. Calc. for $C_{37}H_{32}N_4O_4Zn$: C, 67.1; H, 4.8; N, 8.4; Zn, 9.8%; Found C, 66.8; H, 4.3; N, 8.2; Zn, 9.6%. IR data (KBr, cm^{-1}); 1608 ν(C=N); 1519 ν(−HC=C); 451 (M−N), 531 ν(M−O). MS *m/z* (%): 660 [M^+]. ^{1}H NMR (δ): 6.9–7.45 (aromatic) (m); 2.07 (CH_3, 6H) (s), 3.17 (CH_2) (s), 7.1–9.3 (bpy) (m). ^{13}C NMR (δ, ppm): 127.8–128.6 (C_1 to C_3), 132.9 (C_4), 136.8 (C_5), 110.4 (C_6), 175.4 (C_7), 136.0 (C_8), 127.2–130.0 (C_9–C_{12}), 20.4 (C_{13}), 121–155.3 (C_{14}–C_{18}), 174.2 (C_{19}), 38.1 (C_{20}). Λ_M 10^{-3} (ohm^{-1} cm^2 mol^{-1}) = 11.8. λ_{max} (nm) in DMF, 302, 339. μ_{eff} (BM): diamagnetic.

[CuL(MA)(phen)] (**5**), Yield: 78%, Anal. Calc. for $C_{39}H_{32}CuN_4O_4$: C, 68.4; H, 4.7; Cu, 9.2; N, 8.1%; Found C, 68.2; H, 4.4; Cu, 9.0; N, 7.9%. IR data (KBr, cm^{-1}); 1592 ν(C=N); 1517 ν(−HC=C); 448 (M−N), 533 ν(M−O). MS *m/z* (%):683 [M^+]. Λ_M 10^{-3} (ohm^{-1} cm^2 mol^{-1}) = 23.5. λ_{max} (nm) in DMF, 736, 364, 323. μ_{eff} (BM): 1.87.

[CoL(MA)(phen)] (**6**) Yield: 75%, Anal. Calc. for $C_{39}H_{32}CoN_4O_4$: C, 68.9; H, 4.7; Co, 8.6; N, 8.2%; Found C, 68.6; H, 4.5; Co, 8.3; N, 8.0%. IR data (KBr, cm^{-1}); 1609 ν(C=N); 1529 ν(−HC=C); 439 (M−N), 521 ν(M−O). MS *m/z* (%):679 [M^+]. Λ_M 10^{-3} (ohm^{-1} cm^2 mol^{-1}) = 17.5. λ_{max} (nm) in DMF, 656, 567, 461. μ_{eff} (BM): 4.89.

[NiL(MA)(phen)] (**7**)Yield: 76%, Anal. Calc. for $C_{39}H_{32}N_4NiO_4$: C, 68.9; H, 4.7; N, 8.2; Ni, 8.6%; Found C, 68.5; H, 4.4; N, 8.1; Ni, 8.3%. IR data (KBr, cm^{-1}); 1604 ν(C=N); 1522 ν(−HC=C); 445 (M−N), 516 ν(M−O). MS *m/z* (%):678 [M^+]. Λ_M 10^{-3} (ohm^{-1} cm^2 mol^{-1}) = 13.6. λ_{max} (nm) in DMF, 678,563,446. μ_{eff} (BM): 3.18.

[ZnL(MA)(phen)] (**8**)Yield: 73%, Anal. Calc. for $C_{39}H_{32}N_4O_4Zn$: C, 68.2; H, 4.7; N, 8.1; Zn, 9.5%; Found C, 68.1; H, 4.3; N, 7.9; Zn, 9.3%. IR data (KBr, cm^{-1}); 1598 ν(C=N); 1510 ν(−HC=C); 452 (M−N), 526 ν(M−O). MS *m/z* (%):684 [M^+]. ^{1}H NMR (δ, ppm): 7.3–9.0 (aromatic) (m); 1.7 (CH_3, 6H) (s), 3.17 (CH_2) (s), 8.4–9.1 (phen) (m). ^{13}C NMR (δ, ppm): 127.8–128.6 (C_1 to C_3), 132.9 (C_4), 143.9 (C_5), 108.8 (C_6), 169.3 (C_7), 136.0 (C_8), 127.2–130.0 (C_9–C_{12}), 11.7 (C_{13}), 126–146.7 (C_{14}–C_{18}), 174.2 (C_{19}), 38.1 (C_{20}). Λ_M 10^{-3} (ohm^{-1} cm^2 mol^{-1}) = 22.3. λ_{max} (nm) in DMF, 312, 351. μ_{eff} (BM): diamagnetic.

3. Results and discussion

Scheme 1 portrays the synthetic pathway in the formation of Schiff base and its corresponding complexes. The ligand and its complexes are found to be air stable. The ligand is soluble in common organic solvents but the complexes are soluble only in DMF and DMSO.

3.1. Elemental analysis and molar conductivity measurements

The data obtained from elemental analysis for the metal complexes **1**–**8** agree well with the assigned formulae of the proposed structure showing that all the complexes are in equimolar ratios (Primary ligand: metal: Malonic acid: co-ligand). These mixed ligand complexes are of the type [ML(MA)(bpy)] and [ML(MA)(phen)] wherein L is the Knoevenagel Schiff base; MA is malonic acid; bpy is 2,2′-bipyridine; phen is 1,10-phenanthroline. The metal complexes were dissolved in DMSO, and the molar conductivities of 10^{-3} mol dm^{-3} of the solution at 25 °C were measured. The molar conductance data of the mixed ligand complexes fall within the range (11.8–23.5 Ω^{-1} cm^2 mol^{-1}) that signifies the nature of the complexes to be non-electrolytic [19]. The chloride ion is absent in the ionization sphere of the complexes and is confirmed by the

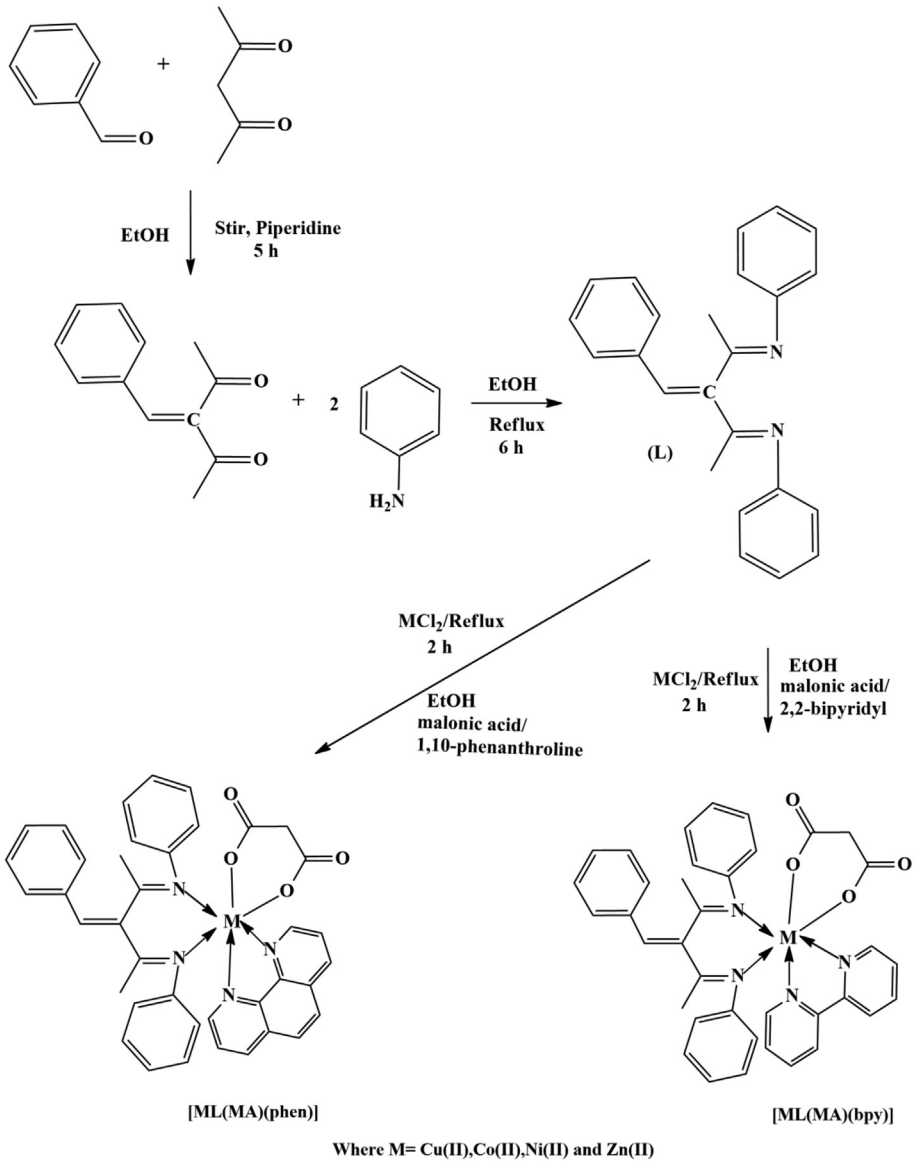

Scheme 1. Synthesis of Schiff base ligand and its metal(II) complexes.

Volhard's test.

3.2. IR spectra

The main aim behind subjecting the metal complexes to FT-IR is to interpret the functionalities present in the complexes formed along with the confirmation of the complexation involved between the metal and ligands. In comparison, the ν(C═N) band present in the ligand spectrum was observed in the region 1609-1584 $cm^{-1}$to be shifted to lower frequency by *ca*.30 cm^{-1}on complexation, indicating that the coordination is through the imine nitrogen [20]. The additional bands in complexes at 1692, 1429 and 924 cm^{-1} could be assigned to the vibrations of the carboxylate moiety. This suggests the denticity of malonic acid to be two and that its coordination to the metal(II) centres *via* the available two monodentate carboxylate groups. These mixed ligand complexes showed the stretching vibration of ν(C═O) of the carboxylate moiety at 1682–1687 cm^{-1}. Comparatively, this high value for this group validates the unsharing of the C═O group in coordination to metal ion and thus the malonate group acts as a dianionic bidentate ligand. Further confirmation is obtained by the formation of metal-oxygen bond ν(M–O) in the complexes in the region 516–533 cm^{-1}. The new band observed in the complexes in the range 437–452 cm^{-1} indicates the formation of metal-nitrogen bond ν(M–N).

3.3. Electronic spectra and magnetic properties of the complexes

The electronic spectral data of the complexes were recorded in DMSO and the spectra are given in supplementary file (Figs. S1–S3). They revealed absorption bands at 380–302 nm where these transitions can be attributed to a charge-transfer band. The slight elevation or decline in the frequency may be attributed to the coordination of the ligand with the metal ions.

The geometry of the complexes **1** and **5** is depicted to be distorted octahedral geometry around the central metal ion as they exhibit d-d transition bands in the range 736–316 nm with $^2E_g \rightarrow {}^2T_{2g}$ as the assigned transition which certainly is the

characteristic of the deduced distorted octahedral geometry. It is further supported by the observed magnetic moment 1.83 and 1.87 BM respectively, thereby instilling its mononuclear d^9 system with S = ½ spin state. This is also in accordance with the microanalytical and mass spectral data. The complexes **2** and **6** displayed three d-d bands in the region 667–441 nm assigned to $^4T_{2g}$ (F)→$^4T_{2g}$(F), $^4T_{1g}$ (F)→$^4A_{2g}$(F) and $^4T_{1g}$ (F)→$^4T_{2g}$(P) transitions, the characteristic of octahedral geometry and supported by the observed magnetic moment values 4.85 and 4.89 BM, at room temperature signifying the monomeric nature of the complexes. Three low intensity bands were observed in the region around 683–427 nm, assigned to transitions $^3A_{2g}$(F)→$^3T_{2g}$(F), $^3A_{2g}$(F)→$^3T_{1g}$(F) and $^3A_{2g}$(F) →$^3T_{1g}$(P) which implied the geometry of Ni(II) ion as octahedral. Furthermore, the observed magnetic moment of the complexes **3** and **7** (3.15 and 3.18 BM respectively) at room temperature indicated the non-coupled mononuclear complexes of a diluted d^8 system with an s = 1 spin state of octahedral geometry [21,22]. The Ni(II) complexes were monomeric in nature which was evidenced by the microanalytical data. The electronic absorption spectra of the diamagnetic Zn(II) complexes (**4** and **8**) showed bands in the region 302–351 nm which were allotted to intraligand charge-transfer transitions [23]. Thus, according to the empirical formulae, the proposed geometry for the Zn(II) complexes is octahedral.

3.4. ^{1}H NMR and ^{13}C NMR spectral analysis

The structural information regarding the synthesized metal complexes can be deduced from the ^{1}H NMR and ^{13}C NMR spectra and their relevant chemical shifts. The ^{1}H NMR spectra of the complexes **4** and **8** are given in Fig. S4. The appearance of multiplet peaks at 6.9–9.3 ppm suggests the presence of aromatic group in the synthesized compounds. The aliphatic methyl protons exhibit a peak at 1.07 and 2.1 ppm for the Zn(II) complexes **4** and **8**. No other appreciable changes can be found in the other signals of the complexes.

Similarly, the ^{13}C NMR spectra of the aromatic carbons in the ligand showed peaks at 119–129 ppm. Also the C═N carbons exhibited downfield shift from 160 ppm to 169 ppm from the ligand to the Zn(II) complexes (**4** and **8**) (Fig. S5). The observed downfield shift suggests the involvement of C═N in the complexation. Furthermore, it confirms the coordination formed and also the proposed formula. No significant changes were found in the other signals.

3.5. Electron paramagnetic spectra of Cu(II) complexes

The EPR spectrum is an ideal technique for studying the environment surrounding the Cu(II) ion. The complexes **1** and **5** were recorded in DMSO at 300 K and 77 K which were then analyzed and the spin Hamiltonian and orbital reduction parameters were calculated and presented in Table 1. The interpretation of the obtained data implies an intense absorption band in the high field and was suggested to be isotropic owing to the tumbling motion of the molecules. Further, three well resolved peaks were detected at Liquid Nitrogen Temperature (LNT) in the low field region. Overall, the spectral data summarize that d^{22}_{x-y} is the ground state for the complexes **1** and **5** which is a characteristic of octahedral geometry and they are also axially symmetric as $A_{||}$ (152) > $A_{\perp}$(114); $g_{||}$ (2.24) > $g_{\perp}$(2.06)> g_e(2.0023) (for complex **5**). Moreover, in an axial symmetry, the expression G = $(g_{||}-2)/(g_{\perp}-2)$ measures the exchange interaction between the copper centres in polycrystalline solid along with the g-values. The G values for **1** and **5** are 4.6 and 4.2 respectively and according to Hathaway [24] they indicate the negligible Cu–Cu exchange interaction in the complexes and their magnetic moment values, 1.83 and 1.87 BM extend further support.

Table 1
The spin Hamiltonian parameters of the Cu(II) complexes in DMSO solution at 77 K.

Complexes	g-tensor			A × 10^{-4} (cm^{-1})			f	G	α^2	β^2
	$g_{||}$	$g_{\perp}$	g_{iso}	$A_{||}$	$A_{\perp}$	A_{iso}				
1	2.22	2.05	2.11	168	122	137	132	4.6	0.84	0.66
5	2.24	2.06	2.12	152	114	126	147	4.2	0.87	0.69

The Kivelson and Neiman equations were employed to calculate the covalency parameters α^2 (covalent in-plane σ-bonding) and β^2 (covalent in-plane π-bonding) [25]. From the table, it is observed that α^2 = 0.84 for complex **1** and 0.87 for complex **5**, indicating considerable covalent character for the metal-ligand bond. Thus, the spectral data discussed above confirm the proposed structure of Cu(II) complexes depicted in Scheme 1.

3.6. Mass spectra

The ESI-mass spectral analysis of the compounds is essential as it is one of the methods to exactly confirm the proposed formula of the synthesized ligands and Cu(II) complexes according to the acquired data. A molecular ion [M^+] peak is observed for the ligand at 338 which is attributed to the ion, $[C_{24}H_{22}N_2]^+$ and the observed other fragments were $[C_6H_7N_2]^{3+}$, $[C_6H_5]^+$ and $[C_5H_6]^{6+}$ at peaks *m/z* 107, 77 and 66 respectively. The mass spectra of [CuL(MA)(bpy)] and [CuL(MA)(phen)] showed peaks at *m/z* 659 and 683 respectively which are the molecular ion peaks. They give a set of fragment peaks at *m/z* 557, 401, 156, 102 which are ascribed to $[C_{34}H_{30}CuN_2]^{2+}$, $[C_{24}H_{22}CuN_2]^{2+}$, $[C_{10}H_8N_2]$ and $[C_3H_2O_4]^{2+}$ respectively. The fragmentations continue further and the demetallation leaves with only the ligand **L** which is 338. The trends of the fragments have point out that the complexes formed are of type [ML(MA)(coligand)] and is concurrent with the IR, NMR data. Thus, in accordance with the mass spectral data and elemental analyses data, the complexes are in equimolar ratio (Fig. S6).

3.7. DNA binding studies

3.7.1. Absorption spectral titrations

Monitoring the affinity of the metal complexes with CT-DNA using absorption spectroscopy is also useful in inferring the binding mode of these compounds. It is crucial as DNA has become an important cellular target and the potential to bind with it, makes way for developing a strong nuclease agent. The interaction of metal complexes with DNA usually occurs *via* both covalent and non-covalent pathways. If the labile ligand of the complexes binds covalently to the nitrogenous base of DNA like guanine N7, it is covalent interaction, whereas the non-covalent DNA binding deals with intercalative, electrostatic and groove binding of metal complexes to the DNA double helix [26]. The absorption spectral data of the complexes in the absence and presence of CT DNA at different concentrations were explored and given in Fig. 1. The metal complexes exhibited an intense absorption around 320–345 nm, attributed to the $n-\pi^*$ transitions. Hypochromicity is observed in the data with the increase in concentration of DNA along with trivial red shift which was found to be in the range 7.0–27.8% and 0.5–4 nm, respectively. When hypochromism and red shift are observed, then the mode of binding is said to be intercalation and is due to the π stacking of the aromatic phenyl rings between the DNA base pairs [27–29]. The binding strength of the complexes was quantified by intrinsic binding constant, (K_b) for the complexes which was evaluated by the change observed in the absorbance values with the increase in the DNA concentration, the values of

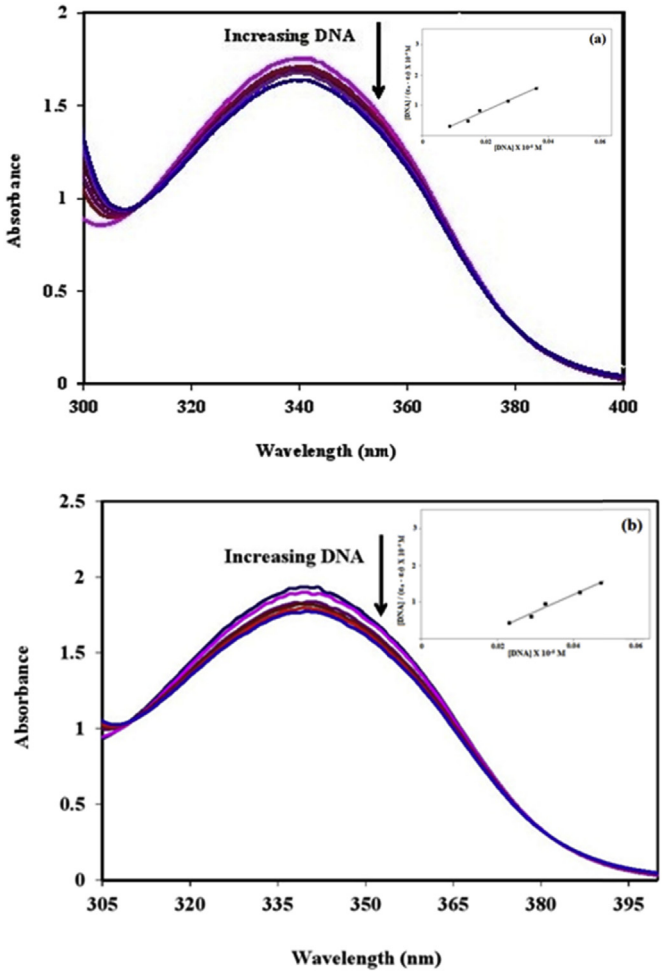

Fig. 1. Absorption spectra of complexes **1** (a) and **5** (b) in buffer pH = 7.2 at 25 °C in presence of increasing amount of DNA where [DNA] = 10^{-3} M. Inset: Plot of [DNA]/($\varepsilon_a-\varepsilon_f$) *vs* [DNA] for complexes **1** and **5** where $K_b = 6.3 \times 10^5$ M^{-1} and 6.6×10^5 M^{-1} respectively.

Table 2
Electronic absorption spectral properties of synthesized compounds.

Complexes	λ_{max} (nm)		Δλ (nm)	[a]H%	[b]K_b (M^{-1})[c]
	Free	Bound			
Ligand	320.5	320.0	0.5	7.0	0.6×10^3
1	342.0	339.0	3.0	25.3	6.3×10^5
2	336.0	332.0	4.0	19.7	5.8×10^5
3	326.0	324.0	2.0	18.0	5.4×10^5
4	331.0	329.0	2.0	16.2	4.8×10^5
5	344.0	341.0	3.0	27.8	6.6×10^5
6	345.0	343.0	2.0	20.5	6.0×10^5
7	338.0	334.0	4.0	17.6	5.7×10^5
8	343.0	340.0	3.0	16.8	5.1×10^5

[a] H% = $[(A_{free}-A_{bound})/A_{free}] \times 100\%$, where H% is the percentage of hypochromicity.
[b] K_b = Intrinsic DNA binding constant determined from the UV–Vis absorption spectral titration.
[c] Error limit ± 3%.

which are displayed in Table 2.

Nevertheless, the metal ions also play a significant role in DNA binding of these complexes along with the effective co-ligands. The binding strength of the complexes is shown as in the following order: **5** > **1**>**6** > **2**>**7** > **3**>**8** > **4**. A strong hypochromism was exhibited by complex **5** along with a slight red shift which is when compared to the other complexes highlights the higher DNA binding propensity of the said complex. The intrinsic binding constant values of the complexes are greater in magnitude ($4.8–6.6 \times 10^5$ M^{-1}) as compared to our previously synthesized complexes, which was achieved between the range ($1.9–4.7 \times 10^6$ M^{-1}) [18]. The reason may be ascribed to the presence of 1,10 phenanthroline and 2,2 bipyridyl that act as chromophore thereby not only facilitating the π stacking between the DNA base pairs but also the coupling of π^* orbital of the intercalated compound with the π orbital of the DNA bases [30]. Hence, the results conclude that the complexes act as strong intercalators. The obtained outcome is due to the presence of the intercalative ligands with extended aromatic plane and the resulting good conjugation effect can significantly support the DNA binding ability.

3.7.2. *Fluorescence spectroscopic studies*

Spectrofluorimetric method is sensitive, easy and has a short analysis time [31,32]. Therefore, it is commonly used in macromolecule-ligand interactions. Considering the previous assumption regarding the contribution of π-stacking between the DNA base pairs towards the observed interactions, ethidium bromide (EB) quenching studies were performed. To the pre-treated DNA-EB system, the metal complexes (solution in DMSO) were added incrementally and their emissions were noted and analyzed. As it is a known fact that EB is a very good intercalator, the rate and intensity of the quenching observed in the emission discloses the binding mode of the metal complex with CT-DNA [33]. Thus, emission spectra of EB bound to DNA in the absence and in the presence of complexes were recorded. The decrease in the emission intensity before and after the addition of metal complex accentuates the fact that the metal complexes are intercalators, as they displace EB in the EB-DNA system causing the gradual decrease in the fluorescence emission. The absorption spectral data of the complexes suggest that their binding affinity found to be $4.8–6.6 \times 10^5$, implies strong intercalation which may be the reason behind the decrease in the emission intensity after the addition of metal complexes. As the binding affinity of the metal complexes to DNA is high, it easily replaces EB thereby resulting in quenching. The binding ability of the copper complexes **1** and **5** was assessed by the EB-DNA compound system and is given in Fig. 2.

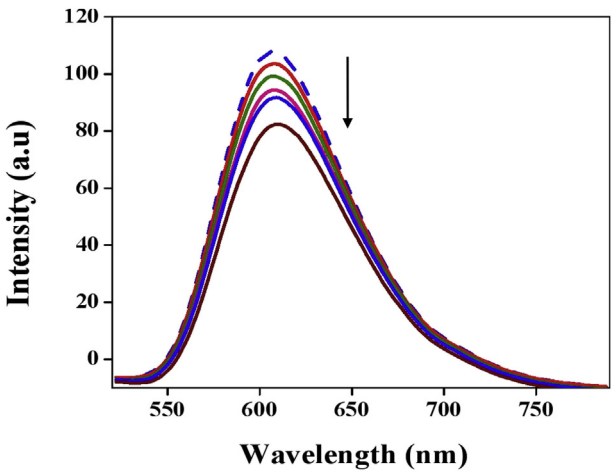

Fig. 2. Emission spectrum of complex **5** in the EB-DNA system with [EB] = 3.3 μM, [DNA] = 20 μM, [complex] = 0–25 μM, λ_{ex} = 500 nm.

3.7.3. Viscosity measurements

Though optical photophysical methods are employed to monitor the binding mode of the metal complex with the DNA, hydrodynamic measurements are preferred as the confirmation tests in the absence of crystallographic data [34]. Generally, the binding mode is interpreted by the increase and decrease of viscosity of the CT-DNA after addition of metal complex. The increase in the viscosity implies the metal complex intercalation between the DNA base pairs that causes the unwinding and lengthening of the said DNA and decrease in the viscosity vouches for the non-classical intercalation binding modes such as groove and electrostatic binding. This unwinding of the DNA strand occurs due to the stacking of the planar ligands between the base pairs is because of the metal complexes acting as metallointercalators, thereby causing a major change in the structure change of the DNA. The van der Waals forces present between the base pairs of the helix are pushed apart due to the intercalating ligands so as to accommodate it [35]. Fig. 3 depicts the observed increase in the DNA viscosity after the increase in the concentration of metal complex due to its consecutive addition. The figure clearly represents that the metal complexes are good metallointercalators with complex **5** being highly effective than the others. Also, the complexes with 1,10 phenanthroline as a coligand show better activity than the others implying the role of aromatic planarity as an important constituent for an effective metallointercalator.

3.7.4. Cyclic voltammetry

The electrochemical investigations are complementary to the earlier used methods of analysis like absorption spectral titration and viscosity measurements [36]. The cyclic voltammograms for complexes **1** and **5** in the presence and absence of varying concentrations of DNA are shown in Fig. 4. With the addition of CT-DNA to the complexes, the voltammetric current coupled with positive shift in $E_{1/2}$ is observed to decrease significantly. The redox potential profiles for interaction of DNA with synthesized compounds are given in Table 3. When the complex binds with DNA, a non-electroactive product is formed which decreases the concentration of the electroactive species present in the solution thereby causing a drop in the peak current [37]. In this case, the fall in voltammetric current when DNA was present may be ascribed to the slow diffusion of the metal complex bound to CT DNA. The positive shift of E_{pc} or E_{pa} indicates that the complex intercalates into DNA double helix, whereas the shift in negative direction specifies groove binding [38,39].

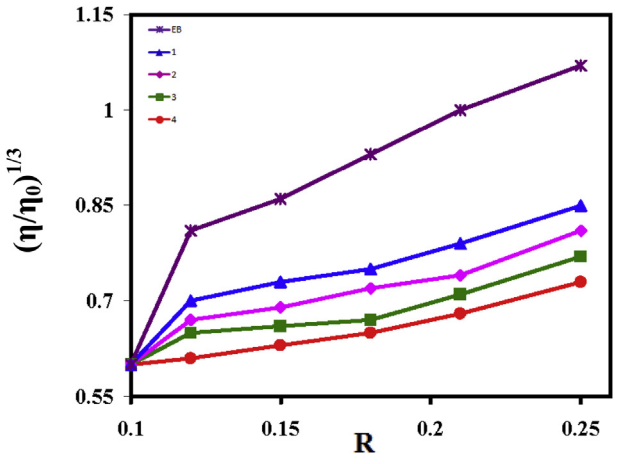

Fig. 3. Effect of increasing amounts of **[EB]** (✱), **1**(▲), **2**(◆), **3**(■), **4**(●) on the viscosity of DNA. R = [complex]/[DNA] or [EB]/[DNA].

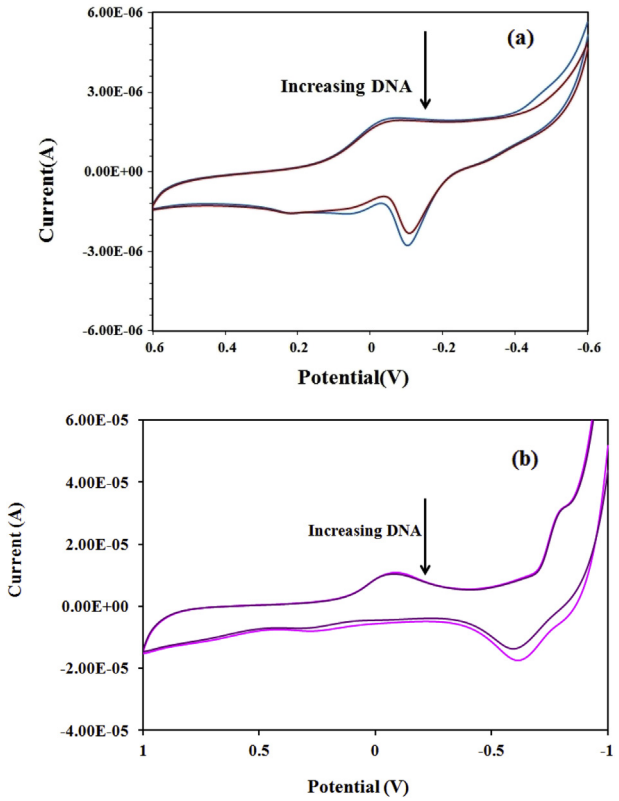

Fig. 4. Cyclic voltammograms of **1** (a) and **5** (b) complexes in buffer pH = 7.2 at 25 °C in presence of increasing amount of DNA. [DNA] = 10^{-3} M.

Table 3
Redox potential profiles for interaction of DNA with synthesized compounds.

Complexes	[a]ΔEp (V)		[b]$E_{1/2}$ (V)		I_{pa}/I_{pc}
	Free	Bound	Free	Bound	
1	0.046	0.598	0.319	0.996	0.73
	−0.409	−0.758	1.997	1.168	0.76
2	0.687	0.584	0.321	0.392	0.66
3	1.871	1.952	0.364	0.425	0.63
4	1.841	1.913	0.285	0.355	0.67
5	0.326	0.572	−1.312	−1.267	0.75
6	1.979	2.171	0.568	0.739	0.62
7	2.428	2.446	0.331	0.324	0.56
8	1.561	1.569	−0.708	−0.682	0.88

Data from cyclic voltammetric measurements: [a]ΔEp = Ep_a−Epc; [b]$E_{1/2}$ is calculated as the average of anodic (E_{Pa}) and cathodic (Ep_c) peak potentials; [b]$E_{1/2} = Ep_a + Epc/2$.

3.8. DNA cleavage efficacy

The efficacy of the metal complexes to act as artificial nucleases is monitored by subjecting the supercoiled plasmid DNA pBR322 to agarose gel electrophoresis. The otherwise supercoiled DNA is said to relax into nicked form and linear form due to the double strand cleavage by the metal complexes. The Fig. 5a displays the cleavage pattern of pBR322 DNA in the presence of metal complexes and H_2O_2. The metal complexes (**5**–**8**) with higher conjugation showed good activity than the other complexes. The lack of DNA cleavage was detected for the control in which the metal complex was absent (lane 1) and in presence of MCl_2 (100 μm) salts (lanes 2–5), illustrated through another Fig. 5b. It can be clearly noted that the lanes 1–9 in Fig. 5a, containing metal complexes (in form I) are converted into form II and form III which are open circular and linear form respectively. The activity of the complexes was

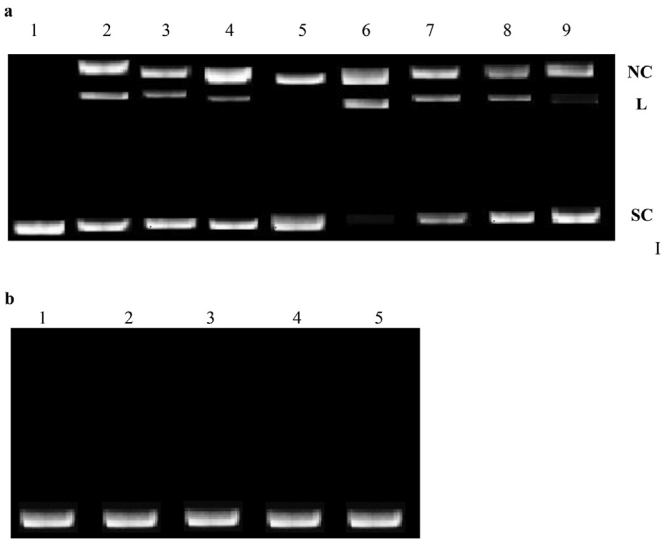

Fig. 5. a. Gel electrophoresis pattern showing cleavage of pBR322 supercoiled DNA (10 μM) in the presence of H_2O_2 (100 μM). Lane 1: DNA control (10 μM); lane 2: DNA+ **1** (60 μM)+H_2O_2; lane 3: DNA+ **2** (60 μM)+H_2O_2; lane 4: DNA+ **3** (60 μM)+H_2O_2; lane 5: DNA+ **4** (60 μM)+H_2O_2; lane 6: DNA+ **5** (60 μM)+H_2O_2; lane 7: DNA+ **6** (60 μM)+H_2O_2; lane 8: DNA+ **7** (60 μM)+H_2O_2; lane 9: DNA+ **8** (60 μM)+H_2O_2. bGel electrophoresis pattern of pBR322 DNA with metal chloride salts. Lane 1: DNA control; Lane 2: DNA + $CuCl_2$ (100 μM); Lane 3: DNA + $CoCl_2$ (100 μM) Lane 4: DNA + $NiCl_2$ (100 μM); Lane 5: DNA + $ZnCl_2$ (100 μM).

appreciably increased in presence of the oxidant. This increase may be observed as a result of the hydrolytic damage to DNA caused by the formation of reactive oxygen species. On the whole, the generation of the reactive oxygen species might be due to the oxidation of hydroxyl free radicals from +2 to +3 presumably through Fenton-type reaction [40]. From these results, we deduce that all the metal complexes **1**–**8** act as potential nuclease agents.

3.9. Antimicrobial activity

Antimicrobial activity for the complexes **1**–**8** was tested *in vitro* against 5 bacterial and 5 fungal strains using broth microdilution method [41]. Their activity was evaluated against standard drugs Kanamycin and Fluconazole. The results are reproduced in Tables 4 and 5. The minimum inhibitory concentration for complex **5** is small suggesting its high biological efficacy. The reason can be explained based on the Overtone's concept [42] and Tweedy's Chelation theory [43]. The polarity of the metal ion decreases after the chelation owing to the overlap of the planar ligand orbitals which causes increase in the delocalization of π-electrons over the whole chelate ring. This consecutively enhances the penetration of the complexes into lipid membranes thereby blocking the metal binding sites in the enzymes of the microorganisms, resulting in the desired activity [44]. The order of the activity is given as follows: **5** > **1**>**6** > **2**>**7** > **3**>**8** > **4**. The order of activity undoubtedly points out that the coligands play an important role in the biological activity. The complexes with highly conjugative 1, 10-phenanthroline as the coligand showed good potential as compared to the 2, 2′-bipyridine conjugated complexes. Thus it can be concluded that more the conjugation, higher the effectiveness of the metal complex.

Table 4
Minimum inhibitory concentration of the synthesized compounds against growth of bacteria (μM).

Compound	Minimum inhibitory concentration (MIC) ($\times 10^4$ μM) [b]SEM = ±2				
	Staphylococcusaureus	*Bacillus subtilis*	*Escherichia coli*	*Klebsiella pneumoniae*	*Salmonella typhi*
L	17.0	18.2	16.3	16.4	16.8
1	8.4	8.7	8.8	8.9	9.3
2	8.9	9.2	9.6	10.1	10.4
3	10.3	10.5	10.9	11.3	11.5
4	11.3	11.9	12.7	13.3	14.1
5	8.1	8.4	8.5	8.3	8.7
6	8.6	8.8	9.1	9.5	9.9
7	9.4	9.6	9.9	10.3	10.8
8	10.7	11.4	11.9	12.5	13.1
[a]Kanamycin	1.6	2.8	1.4	2.3	2.6

[a] Kanamycin is used as the standard.
[b] SEM = Standard Error of Mean.

Table 5
Minimum inhibitory concentration of the synthesized compounds against the growth of fungi (μM).

Compound	Minimum inhibitory concentration (MIC) ($\times 10^4$ μM) [b]SEM = ±2				
	Aspergillus niger	*Fusarium solani*	*Curvularia lunata*	*Rhizoctonia bataticola*	*Candida albicans*
L	18.9	18.5	17.6	15.8	17.6
1	9.7	10.5	11.1	11.4	11.6
2	10.3	11.0	11.9	11.8	12.0
3	10.9	11.8	12.7	12.6	12.9
4	11.5	12.5	13.1	13.0	13.4
5	9.5	9.8	10.5	11.0	11.2
6	9.9	10.8	11.3	11.7	11.8
7	10.6	11.4	12.4	12.3	12.5
8	11.3	12.1	12.9	12.8	13.6
[a]Fluconazole	1.4	1.7	1.2	1.5	1.8

[a] Fluconazole is used as the standard.
[b] SEM = Standard Error of Mean.

4. Conclusion

In the current studies, few mixed ligand metal(II) complexes have been synthesized. They were characterized by IR, UV–Vis., EPR and NMR spectral and micro analytical data and confirmed the stoichiometry of Cu(II), Co(II), Ni(II) and Zn(II) complexes to be equimolar (1: 1: 1 (M: L: coligand)) that adopt octahedral geometry. The other investigations like DNA binding with CT DNA and antimicrobial screening accentuate the higher activity exhibited by the Cu(II) complexes, especially **5** which has a highly conjugative planar ligand, 1,10-phenanthroline in its environment that binds through intercalation. The studies undertaken also confirm the valuable contribution of the conjugated planar ligands along with the chelation which plays a vital role in designing of potent antimicrobial agents. The results of the investigations carried out in this study, compared to our previous studies [18], show profound increase in the DNA binding constant and DNA interaction studies along with antimicrobial activity. The complexes can be fine tuned to make them into better antimicrobial agents and DNA probes.

Acknowledgment

The authors express their heartfelt thanks to the Science and Engineering Research Board (SERB), DST (File No.SR/S1/IC-27/2012), New Delhi, India for financial Support. They also express their gratitude to the College Managing Board, Principal and Head of the Department of Chemistry, VHNSN College, Virudhunagar for providing research facilities.

Appendix A. Supplementary data

Supplementary data related to this article can be found at http://dx.doi.org/10.1016/j.molstruc.2016.06.034.

References

[1] (a) E. Meggers, From conventional to unusual enzyme inhibitor scaffolds: the quest for target, Angew. Chem. Int. Ed. 50 (2011) 2442–2448;
(b) G. Sava, G. Jaouen, E.A. Hillard, A. Bergamo, Targeted therapy vs. DNA-adduct formation-guided design: thoughts about the future of metal-based anticancer drugs, Dalton Trans. 41 (2012) 8226–8234;
(c) C.G. Hartinger, N. Metzler-Nolte, P.J. Dyson, Challenges and opportunities in the development of organometallic anticancer drugs, Organometallics 31 (2012) 5677–5685;
(d) N.P. Barry, P.J. Sadler, Exploration of the medical periodic table: towards new targets, Chem. Commun. 49 (2013) 5106–5131.

[2] (a) E.R. Jamieson, S.J. Lippard, Structure, recognition, and processing of cisplatin-DNA adducts, Chem. Rev. 99 (1999) 2467–2498;
(b) E. Wong, C.M. Giandomenico, Current status of platinum-based antitumor drugs, Chem. Rev. 99 (1999) 2451–2466;
(c) C.X. Zhang, S.J. Lippard, New metal complexes as potential therapeutics, Curr. Opin. Chem. Biol. 7 (2003) 481–489;
(d) Y. Wang, Q.Y. He, R.W. Y.Sun, C.M. Che, J.F. Chiu, Cellular pharmacological properties of gold(III) porphyrin 1a, a potential anticancer drug lead, Eur. J. Pharmacol. 554 (2007) 113–122.

[3] (a) V. Rajendiran, M. Murali, E. Suresh, S. Sinha, K. Somasundaram, M. Palaniandavar, Mixed ligand ruthenium(II) complexes of bis(pyrid-2-yl)-/bis(benzimidazol-2-yl)-dithioether and diimines: study of non-covalent DNA binding and cytotoxicity, Dalton Trans. (2008) 148–163;
(b) B. Neto, A. Lapis, Recent developments in the chemistry of deoxyribonucleic acid (DNA) intercalators: principles, design, synthesis, applications and trends, Molecules 14 (2009) 1725–1746.

[4] L. Strekowski, B. Wilson, Noncovalent interactions with DNA: an overview, Fundam. Mol. Mech. Mutagen 623 (2007) 3–13.

[5] (a) M. Navarro, E.J. Cisneros-Fajardo, A. Sierralta, M. Ferna'ndez-Mestre, P. Silva, D. Arrieche, E. Marchan, Design of copper DNA intercalators with leishmanicidal activity, J. Biol. Inorg. Chem. 8 (2003) 401–408;
(b) M.S. Deshpande, A.A. Kumbhar, S. Kumbhar, A.M. Kumbhakar, H. Pal, U.B. Sonawane, R.R. Joshi, Ruthenium (II) complexes of bipyridine– glycoluril and their interactions with DNA, Bioconjugate Chem. 20 (2009) 447–459.

[6] J. Jiang, X. Tang, W. Dou, H. Zhang, W. Liu, C. Wang, J. Zheng, Synthesis and characterization of the ligand based on benzoxazole and its transition metal complexes: DNA-binding and antitumor activity, J. Inorg. Biochem. 104 (2010) 583–591.

[7] (a) D. Kong, J. Reibenspies, J. Mao, A. Cleafield, A.E. Martell, Novel 30-membered octaazamacrocyclic ligand: synthesis, characterization, thermodynamic stabilities and DNA cleavage activity of homodinuclear copper and nickel complexes, Inorg. Chim. Acta 342 (2003) 158–170;
(b) S. Budagumpi, N.V. Kulkarni, G.S. Kurdekar, M.P. Sathisha, V.K. Revankar, Synthesis and spectroscopy of Co(II), Ni(II), Cu(II) and Zn(II) complexes derived from 3, 5-disubstituted-1H-pyrazole derivative: a special emphasis on DNA binding and cleavage studies, Eur. J. Med. Chem. 45 (2010) 455–462.

[8] (a) S. Anbu, R. Ravishankaran, A.A. Karande, M. Kandaswamy, DNA targeting polyaza macrobicyclic dizinc (II) complexes promoting high in vitro caspase dependent anti-proliferative activity against human carcinoma cancer cells, Dalton Trans. 41 (2012) 12970–12983.

[9] A.A. Moosavi-Movahedi, A.R. Golchin, K. Nazari, J. Chamani, A.A. Saboury, S.Z. Bathaie, S. Tangestani-Nejad, Microcalorimetry, energetics and binding studies of DNA–dimethyltin dichloride complexes, Thermochim. Acta 414 (2004) 233–241.

[10] E. Rahnama, M. Mahmoodian-Moghaddam, S. Khorsand-Ahmadi, M.R. Saberi, J. Chamani, Binding site identification of metformin to human serum albumin and glycated human serum albumin by spectroscopic and molecular modeling techniques: a comparison study, J. Biomol. Struct. Dyn. 33 (2015) 513–533.

[11] J. Chamani, Energetic domains analysis of bovine α-lactalbumin upon interaction with copper and dodecyl trimethylammonium bromide, J. Mol. Struct. 979 (2010) 227–234.

[12] Z. Sattar, M.R. Saberi, J. Chamani, Determination of LMF binding site on a HSA-PPIX complex in the presence of human holo transferrin from the viewpoint of Drug Loading on Proteins, PLoS One (2014), http://dx.doi.org/10.1371/journal.pone.0084045.

[13] (a) N. Shahabadi, S. Kashanian, F. Darabi, DNA binding and DNA cleavage studies of a water soluble cobalt(II) complex containing dinitrogen Schiff base ligand: the effect of metal on the mode of binding, Eur. J. Med. Chem. 45 (2010) 4239–4245;
(b) C. Tolia, A.N. Papadopoulos, C.P. Raptopoulou, V. Psycharis, C. Garino, L. Salassa, G. Psomas, Copper(II) interacting with the non-steroidal antiinflammatory drug flufenamic acid:Structure, antioxidant activity and binding to DNA and albumins, J. Inorg. Biochem. 123 (2013) 53–65.

[14] A. Jayamani, V. Thamilarasan, N. Sengottuvelan, P. Manisankar, S.K. Kang, Y. Kim, V. Ganesan, Synthesis of mononuclear copper(II) complexes of acyclic Schiff's base ligands: spectral, structural, electrochemical, antibacterial, DNA binding and cleavage activity, Spectrochim. Acta A 122 (2014) 365–374.

[15] (a) S.D. Joshi, D. Kumar, S.R. Dixit, N. Tigadi, U.A. More, C. Lherbet, T.M. Aminabhavi, K.S. Yang, Synthesis, characterization and antitubercular activities of novel pyrrolyl hydrazones and their Cu-complexes, Eur. J. Med. Chem. 121 (2016) 21–39;
(b) O.G. Idemudia, A.P. Sadimenko, E.C. Hosten, Metal complexes of new bioactive pyrazolone phenylhydrazones; crystal structure of 4-acetyl-3-methyl-1-phenyl-2-pyrazoline-5-one phenylhydrazone Ampp-Ph, Int. J. Mol. Sci. (2016), http://dx.doi.org/10.3390/ijms17050687;
(c) A. Alsalme, S. Laeeq, S. Dwivedi, M.S. Khan, K. Al Farhan, J. Musarrat, R.A. Khan, Synthesis, characterization of α-amino acid Schiff base derived Ru/Pt complexes: induces cytotoxicity in HepG2 cell via protein binding and ROS generation, Spectrochim. Acta A 163 (2016) 1–7.

[16] S.T. Chew, K.M. Lo, S.K. Lee, M.P. Heng, W.Y. Teoh, K.S. Sim, K.W. Tan, Copper complexes with phosphonium containing hydrazone ligand: topoisomerase inhibition and cytotoxicity study, Eur. J. Med. Chem. 76 (2014) 397–407.

[17] (a) N. Pravin, N. Raman, Investigation of *in vitro* anticancer and DNA strap interactions in live cells using carboplatin type Cu(II) and Zn(II) metal-loinsertors, Eur. J. Med. Chem. 85 (2014) 675–687;
(b) N. Raman, N. Pravin, DNA fastening and ripping actions of novel Knoevenagel condensed dicarboxylic acid complexes in antitumor journey, Eur. J. Med. Chem. 80 (2014) 57–70;
(c) N. Pravin, V. Devaraji, N. Raman, Targeting protein kinase and DNA molecules by diimine–phthalate complexes in antiproliferative activity, Int. J. Biol. Macromol. 79 (2015) 837–855.

[18] N. Raman, N. Pravin, Lasing the DNA fragments through β-diketimine framed Knoevenagel condensed Cu (II) and Zn (II) complexes–An in vitro and in vivo approach, Spectrochim. Acta A 118 (2014) 867–882.

[19] W.G. Geary, The use of conductivity measurements in organic solvents for the characterisation of coordination compounds, Coord. Chem. Rev. 7 (1971) 81–122.

[20] K. Nakamato, Infrared and Raman Spectra of Inorganic and Coordination Compounds, fourth ed., Wiley, New York, 1986.

[21] F.A. Cotton, G. Wilkinson, Advanced Inorganic Chemistry, fifth ed., Wiley, New York, 1988.

[22] S.S. Konstantinovic, B.C. Radovanovic, A. Krkljes, Thermal behaviour of Co(II), Ni(II), Cu(II), Zn(II), Hg(II) and Pd(II) complexes with isatin-beta-thiosemicarbazone, J. Therm. Anal. Calorim. 90 (2007) 525–531.

[23] N. Raman, K. Pothiraj, T. Baskaran, DNA interaction, antimicrobial, electrochemical and spectroscopic studies of metal (II) complexes with tridentate heterocyclic Schiff base derived from 2′-methylacetoacetanilide, J. Mol. Struct. 1000 (2011) 135–144.

[24] R.K. Ray, G.B. Kauffman, EPR spectra and covalency of bis(amidinourea/O-alkyl-1-amidinourea)copper(II) complexes Part II. Properties of the CuN42– chromophore, Inorg. Chim. Acta 173 (1990) 207–214.

[25] D.X. West, 2-aminopyridine n-oxide complexes formed from various copper(II) salts, Inorg. Nucl. Chem. 43 (1984) 3169–3174.

[26] M. Baldini, M. Belicchi-Ferrari, F. Bisceglie, P.P. Dall'Aglio, G. Pelosi, S. Pinelli, P. Tarasconi, Copper(II) complexes with substituted thiosemicarbazones of α-ketoglutaric acid: synthesis, X-ray structures, DNA binding studies, and nuclease and biological activity, Inorg. Chem. 43 (2004) 7170–7179.
[27] J.M. Kelly, A.B. Tossi, D.J. McConnell, C.O. Uigin, A study of the interactions of some polypyridylruthenium(II) complexes with DNA using fluorescence spectroscopy, topoisomerisation and thermal denaturation, Nucleic Acids Res. 13 (1985) 6017–6034.
[28] A.M. Pyle, J.P. Rehmann, R. Meshoyrer, C.V. Kumar, N.J. Turro, K.K. Barton, Mixed-ligand complexes of ruthenium(II): factors governing binding to DNA, J. Am. Soc. Chem. 111 (1989) 3051–3058.
[29] H. Chao, W.J. Mei, Q.W. Huang, L.N. Ji, DNA binding studies of ruthenium (II) complexes containing asymmetric tridentate ligands, J. Inorg. Biochem. 25 (2002) 165–170.
[30] S. Tabassum, S. Amir, F. Arjmand, C. Pettinari, F. Marchetti, N. Masciocchi, G. Lupidi, R. Pettinari, Mixed-ligand Cu(II)-vanillin Schiff base complexes; effect of coligands on their DNA binding, DNA cleavage, SOD mimetic and anticancer activity, Eur. J. Med. Chem 60 (2013) 216–232.
[31] O. Duman, S. Tunc, B.K. Bozoglan, Characterization of the binding of meto-prolol tartrate and guaifenesin drugs to human serum albumin and human hemoglobin proteins by fluorescence and circular dichroism spectroscopy, J. Fluoresc. 23 (2013) 659–669.
[32] S. Tunc, O. Duman, B.K. Bozoglan, Studies on the interactions of chloroquine diphosphate and phenelzine sulfate drugs with human serum albumin and human hemoglobin proteins by spectroscopic techniques, J. Lumin 140 (2013) 87–94.
[33] D.L. Boger, B.E. Fink, M.P. Hedrick, Total synthesis of distamycin A and 2640 Analogues: a solution-phase combinatorial approach to the discovery of new, bioactive DNA binding agents and development of a rapid, high-throughput screen for determining relative DNA binding affinity or DNA binding sequence selectivity, J. Am. Chem. Soc. 122 (2000) 6382–6394.
[34] J. Sun, S. Wu, Y. An, J. Liu, F. Gao, L.-N. Ji, Z.-W. Mao, Synthesis, crystal structure and DNA-binding properties of ruthenium(II) polypyridyl complexes with dicationic 2,2′-dipyridyl derivatives as ligands, Polyhedron 27 (2008) 2845–2850.
[35] L.F. Tan, X.H. Liu, H. Chao, L.N. Ji, Synthesis, DNA-binding and photocleavage studies of ruthenium(II) complex with 2-(3′-phenoxyphenyl)imidazo[4,5-f][1,10]phenanthroline, J. Inorg. Biochem. 101 (2007) 56–63.
[36] F. Boussicault, M. Robert, Electron transfer in DNA and DNA-related biological processes. Electrochemical insights, Chem. Rev. 108 (2008) 2622–2645.
[37] J.M. Kelly, E.G. Lyons, J.M.V. Putten, R.E. Smythm, Analytical Chemistry, Symposium Series, Electrochemistry, Sensors and Analysis, 25, Elsevier, Amsterdam, 1986, pp. 205–212.
[38] S.S. Zhang, S.Y. Niu, B. Qu, G.F. Jie, H. Xu, C.F. Ding, Studies on the interaction mechanism between hexakis(imidazole) manganese(II) terephthalate and DNA and preparation of DNA electrochemical sensor, J. Inorg. Biochem. 99 (2005) 2340–2347.
[39] M.T. Carter, M. Rodriguez, A.J. Bard, Voltammetric studies of the interaction of metal chelates with DNA. 2. Tris-chelated complexes of cobalt(III) and iron(II) with 1,10-phenanthroline and 2,2′-bipyridine, J. Am. Chem. Soc. 111 (1989) 8901–8911.
[40] A.S. Munde, A.N. Jagdale, S.M. Jadhow, T.K. Chondhekar, Synthesis and characterization of some transition metal complexes of unsymmetrical tetradentate Schiff base ligand, J. Korean Chem. Soc. 53 (2009) 407–414.
[41] M. Sonmez, M. Celebi, I. Berber, Synthesis, spectroscopic and biological studies on the new symmetric Schiff base derived from 2, 6-diformyl-4-methylphenol with N-aminopyrimidine, Eur. J. Med. Chem. 45 (2010) 1935–1940.
[42] Y. Anjaneyulu, R.P. Rao, Preparation, characterization and antimicrobial activity studies on some ternary complexes of Cu(II) with acetylacetone and various salicylic acids, Synth. React. Inorg. Met. Org. Chem. 16 (1986) 257–272.
[43] N.N. Al-Mohammed, Y. Alias, Z. Abdullah, R.M. Shakir, E.M. Taha, A.A. Hamid, Synthesis and antibacterial evaluation of some novel imidazole and benzimidazole sulfonamides, Molecules 18 (2013) 11978–11995.
[44] R. Taherlo, M. Salehi, Synthesis, crystal structures, electrochemically studies and antibacterial properties of three new mono-nuclear and one very rare binuclear cobalt(III) Schiff base complexes, Inorg. Chim. Acta 418 (2014) 180–186.